AFRL-VA-WP-TP-2006-347

BASIS CONSTRUCTION FOR THE DESIGN OF BOUNDARY FEEDBACK CONTROLS FROM REDUCED ORDER MODELS (PREPRINT)

R. Chris Camphouse

NOVEMBER 2006

Approved for public release; distribution is unlimited.

STINFO COPY

AIR VEHICLES DIRECTORATE
AIR FORCE MATERIEL COMMAND
AIR FORCE RESEARCH LABORATORY
WRIGHT-PATTERSON AIR FORCE BASE, OH 45433-7542

NOTICE AND SIGNATURE PAGE

Using Government drawings, specifications, or other data included in this document for any purpose other than Government procurement does not in any way obligate the U.S. Government. The fact that the Government formulated or supplied the drawings, specifications, or other data does not license the holder or any other person or corporation; or convey any rights or permission to manufacture, use, or sell any patented invention that may relate to them.

This report was cleared for public release by the Air Force Research Laboratory Wright Site (AFRL/WS) Public Affairs Office and is available to the general public, including foreign nationals. Copies may be obtained from the Defense Technical Information Center (DTIC) (http://www.dtic.mil).

AFRL-VA-WP-TP-2006-347 HAS BEEN REVIEWED AND IS APPROVED FOR PUBLICATION IN ACCORDANCE WITH ASSIGNED DISTRIBUTION STATEMENT.

*//Signature//

R. Chris Camphouse
Mathematician
Control Design and Analysis Branch
Air Force Research Laboratory
Air Vehicles Directorate

//Signature//

Deborah S. Grismer
Chief
Control Design and Analysis Branch
Air Force Research Laboratory
Air Vehicles Directorate

//Signature//

JEFFREY C. TROMP
Senior Technical Advisor
Control Sciences Division
Air Vehicles Directorate

This report is published in the interest of scientific and technical information exchange, and its publication does not constitute the Government's approval or disapproval of its ideas or findings.

*Disseminated copies will show "//Signature//" stamped or typed above the signature blocks.

REPORT DOCUMENTATION PAGE

Form Approved
OMB No. 0704-0188

1. REPORT DATE *(DD-MM-YY)*	2. REPORT TYPE	3. DATES COVERED *(From - To)*
November 2006	Journal Article Preprint	01/01/2006 – 11/01/2006

4. TITLE AND SUBTITLE
BASIS CONSTRUCTION FOR THE DESIGN OF BOUNDARY FEEDBACK CONTROLS FROM REDUCED ORDER MODELS (PREPRINT)

5a. CONTRACT NUMBER
In-house

5b. GRANT NUMBER

5c. PROGRAM ELEMENT NUMBER
60612

6. AUTHOR(S)
R. Chris Camphouse

5d. PROJECT NUMBER
2304

5e. TASK NUMBER
CT

5f. WORK UNIT NUMBER
RL

7. PERFORMING ORGANIZATION NAME(S) AND ADDRESS(ES)

Control Design and Analysis Branch (AFRL/VACA)
Control Sciences Division
Air Vehicles Directorate
Air Force Materiel Command, Air Force Research Laboratory
Wright-Patterson Air Force Base, OH 45433-7542

8. PERFORMING ORGANIZATION REPORT NUMBER
AFRL-VA-WP-TP-2006-347

9. SPONSORING/MONITORING AGENCY NAME(S) AND ADDRESS(ES)

Air Vehicles Directorate
Air Force Research Laboratory
Air Force Materiel Command
Wright-Patterson Air Force Base, OH 45433-7542

10. SPONSORING/MONITORING AGENCY ACRONYM(S)
AFRL-VA-WP

11. SPONSORING/MONITORING AGENCY REPORT NUMBER(S)
AFRL-VA-WP-TP-2006-347

12. DISTRIBUTION/AVAILABILITY STATEMENT
Approved for public release; distribution is unlimited.

13. SUPPLEMENTARY NOTES
Journal article submitted to the Journal of Guidance, Control, and Dynamics, published by AIAA.

PAO Case Number: AFRL/WS 06-2743 (cleared November 06, 2006). Paper contains color.

14. ABSTRACT

We develop a reduced basis construction method that allows for separate consideration of baseline and actuated dynamics in the reduced modeling process. A prototype initial boundary value problem, governed by the two-dimensional Burgers equation, is formulated to demonstrate the utility of the method in a boundary control setting. A weak formulation approach, in combination with proper orthogonal decomposition and Galerkin projection, is used to develop a reduced model of the distributed parameter system. Comparisons are done between reduced and full order solutions under open-loop boundary actuation to illustrate advantages gained by separate consideration of actuated dynamics in the reduced modeling process. A tracking control problem is specified for the full order system using a linear quadratic regulator formulation. Comparisons of feedback control effectiveness are done to demonstrate benefits in control effectiveness obtained from separate consideration of actuated dynamics during model reduction.

15. SUBJECT TERMS

16. SECURITY CLASSIFICATION OF:			17. LIMITATION OF ABSTRACT:	18. NUMBER OF PAGES	19a. NAME OF RESPONSIBLE PERSON (Monitor)
a. REPORT	b. ABSTRACT	c. THIS PAGE			R. Chris Camphouse
Unclassified	Unclassified	Unclassified	SAR	24	19b. TELEPHONE NUMBER *(Include Area Code)* N/A

Standard Form 298 (Rev. 8-98)
Prescribed by ANSI Std. Z39-18

Basis Construction for the Design of Boundary Feedback Controls from Reduced Order Models

R. Chris Camphouse [1]
Control Design and Analysis Branch
Air Vehicles Directorate
Wright-Patterson Air Force Base

Abstract

In this paper, we develop a reduced basis construction method that allows for separate consideration of baseline and actuated dynamics in the reduced modeling process. A prototype initial boundary value problem, governed by the two-dimensional Burgers equation, is formulated to demonstrate the utility of the method in a boundary control setting. A weak formulation approach, in combination with proper orthogonal decomposition and Galerkin projection, is used to develop a reduced model of the distributed parameter system. Comparisons are done between reduced and full order solutions under open-loop boundary actuation to illustrate advantages gained by separate consideration of actuated dynamics in the reduced modeling process. A tracking control problem is specified for the full order system using a linear quadratic regulator formulation. Comparisons of feedback control effectiveness are done to demonstrate benefits in control effectiveness obtained from separate consideration of actuated dynamics during model reduction.

Nomenclature

L	covariance matrix
S	solution snapshot
N	total number of snapshots
T	actuated snapshot
N_A	total number of actuated snapshots
ϕ, α	basis mode and temporal coefficient, respectively
M	total number of basis modes
M_B, M_A	total number of baseline and actuator modes, respectively
ξ, η	baseline and actuator mode, respectively
θ, β	baseline and actuator mode temporal coefficient, respectively
λ, v	eigenvalue and eigenvector, respectively
A, B	state and control matrices, respectively
G, F	nonlinear and forcing matrices, respectively
Q, R	state and control weight matrices, respectively
K	feedback gain matrix
γ	control robustness parameter
Ω	spatial domain
t	time
$\mathbf{x}$	spatial coordinate vector
h	spatial step-size

Introduction

Reduced order modeling has received significant research attention in recent years. For many problems of practical interest, the order of the system describing the application must be reduced. An illustrative example where this is required is the development of feedback control laws for fluid flow configurations. It is not uncommon for discretized flow models to describe millions of state variables.[1] Unfortunately, the development of systematic feedback control laws from systems of such large dimension is a computationally intractable problem. For example, if one uses a linear quadratic regulator (LQR) control formulation, roughly 10^{12} Riccati unknowns need to be calculated for a discretized flow model describing 10^6 states. The Riccati unknowns are solutions to a nonlinear matrix equation.[2] Existing computing power and computational algorithms are not capable of solving an LQR problem of such large dimension. For dynamical models that

[1]Mathematician, Member AIAA
2210 Eighth St., Bldg 146, Room 305
WPAFB OH, 45433

are very large scale, such as those describing fluid flow configurations, it is apparent that the order of the system must be reduced prior to control law design.[3]

Several research efforts have been concerned with, or relied upon, the development of order reduction strategies that provide reduced order models in a form amenable to state-space feedback control law design.[4–14] For the case of boundary control, the development of such models has been an open problem. For many applications of practical interest, such as feedback control of the air flow over an airplane wing, boundary actuation is a requirement. These applications require actuation to be located on the surface if they are to be implemented in hardware in the physical system. Most reduced modeling efforts have either been concerned with the case of control action via a body force or have approximated boundary actuation by a body force on the domain interior. The reduced modeling task is usually simpler in the case of body forcing due to the presence of homogeneous boundary conditions.

Few techniques have been obtained thus far providing reduced order models with explicit boundary input that can be used for systematic design of feedback control laws. The case of boundary actuation is simply more difficult than the case of body forcing. It is difficult to extract the boundary control input in the reduced model. When proper orthogonal decomposition (POD) is used in conjunction with Galerkin projection, boundary conditions are absorbed in the process. An additional step is required to make the action of the control input explicit in the model. Approximating boundary actuation as a body force near the boundary is convenient. It circumvents the difficulty associated with making boundary control inputs explicit in the reduced model. However, feedback control by body forcing is a very different problem mathematically than the problem of boundary control. In the context of systems governed by partial differential equations, boundary control leads to an unbounded control input operator.[15] In other words, when viewed as an operator equation, boundary control leads to an unbounded B operator in the state equation

$$\dot{x} = Ax + Bu, \tag{1}$$

$$x(0) = x_0. \tag{2}$$

For the case of body forcing, the B operator is typically bounded. As a result, while convenient, the reliability associated with approximating a boundary control as a distributed body force is questionable.

Recently, inroads have been made allowing for the extraction of boundary conditions in reduced order POD models. For the most part, these methods utilize POD in combination with a weak formulation of the Galerkin projection.[16–19] The advantage of a weak formulation is that boundary conditions appear naturally when the reduced model is written weakly. In this paper, we utilize a method[16] incorporating difference approximations in the weak formulation to construct reduced models with boundary control input appearing explicitly.

Special care must be taken when POD is used for the development of feedback control laws. For many canonical control formulations, the dynamics induced by the feedback control are not known a priori. Thus, it is difficult to construct a set of POD basis modes capable of spanning the baseline solution as well as the dynamics of the system with boundary actuation. It is entirely possible that the dynamics induced by a feedback control are not adequately represented by the reduced model if the POD basis is not constructed carefully. Construction of a POD basis capable of spanning the baseline solution, as well as dynamics introduced by boundary actuation, is the subject of this paper.

Model Problem

A distributed parameter system is formulated which models convective flow over an obstacle. The resulting model problem is used to demonstrate the importance of careful reduced model design. Let $\Omega_1 \subseteq \mathbb{R}^2$ be the rectangle given by $(a, b] \times (c, d)$. Let $\Omega_2 \subseteq \Omega_1$ be the rectangle given by $[a_1, a_2] \times [b_1, b_2]$ where $a < a_1 < a_2 < b$ and $c < b_1 < b_2 < d$. The problem domain, Ω, is given by $\Omega = \Omega_1 \setminus \Omega_2$. In this configuration, Ω_2 is the obstacle. Dirichlet boundary controls are located on the obstacle bottom and top, denoted by Γ_B and Γ_T, respectively.

The dynamics of the system are described by the two-dimensional Burgers equation

$$\frac{\partial}{\partial t} w(t, x, y) + \nabla \cdot F(w) = \frac{1}{Re} \Delta w(t, x, y) \tag{3}$$

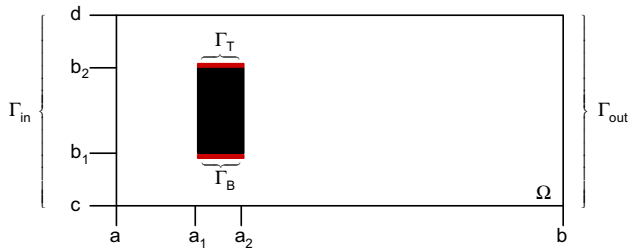

Figure 1: Problem Geometry.

for $t > 0$ and $(x, y) \in \Omega$. In (3), $F(w)$ has the form

$$F(w) = \left[C_1 \frac{w^2(t,x,y)}{2} \qquad C_2 \frac{w^2(t,x,y)}{2} \right]^T, \tag{4}$$

where C_1, C_2 are nonnegative constants. This equation has a convective nonlinearity like that found in the Navier-Stokes momentum equation modeling fluid flow.[20] The quantity Re, a nonnegative constant, is analogous to the Reynolds number in the Navier-Stokes momentum equation.

To complete the model of the system, boundary conditions must be specified as well as an initial condition. For simplicity, boundary controls are assumed to be separable. With this assumption, we specify conditions on the obstacle bottom and top of the form

$$w(t, \Gamma_B) = u_B(t)\Psi_B(x), \tag{5}$$
$$w(t, \Gamma_T) = u_T(t)\Psi_T(x). \tag{6}$$

In (5)-(6), $u_B(t)$ and $u_T(t)$ are the controls on the bottom and top of the obstacle, respectively. The profile functions $\Psi_B(x)$ and $\Psi_T(x)$ describe the spatial influence of the controls on the boundary. A parabolic inflow condition is specified of the form

$$w(t, \Gamma_{in}) = f(y). \tag{7}$$

At the outflow, a Neumann condition is specified according to

$$\frac{\partial}{\partial x} w(t, \Gamma_{out}) = 0. \tag{8}$$

For notational convenience, denote the remaining boundary as Γ_U. We require that values be fixed at zero along Γ_U as time evolves. The resulting boundary condition is of the form

$$w(t, \Gamma_U) = 0. \tag{9}$$

The initial condition of the system is given by

$$w(0, x, y) = w_0(x, y) \in L^2(\Omega). \tag{10}$$

Reduced Basis Construction

In this work, we use a POD algorithm[21] based on the snapshot method[22] to construct the low order basis needed for the development of the reduced order model. A data ensemble of snapshots $\{S_i(\mathbf{x})\}_{i=1}^N$ is generated for the system via numerical simulation or experiment, where N is the total number of snapshots. Each snapshot consists of instantaneous system data. With the snapshot ensemble in hand, the $N \times N$ correlation matrix L defined by

$$L_{i,j} = \langle S_i, S_j \rangle \tag{11}$$

is constructed. In this work, we utilize the standard $L^2(\Omega)$ inner product

$$\langle S_i, S_j \rangle = \int_\Omega S_i S_j^* \mathbf{dx}, \tag{12}$$

where S_j^* denotes the complex conjugate of S_j, in the construction of L.

The eigenvalues $\{\lambda_i\}_{i=1}^N$ of L are calculated and sorted in descending order. The ratio

$$100\left(\frac{\sum_{i=1}^M \lambda_i}{\sum_{i=1}^N \lambda_i}\right) \tag{13}$$

is used to determine the number of POD basis functions to construct. The quantity in (13) provides a measure of the ensemble energy that is captured by a POD basis consisting of M modes. By requiring a percentage of the energy contained in the snapshot ensemble be contained in the basis, the smallest value of M is calculated such that the quantity in (13) is greater than or equal to that percentage.

The eigenvectors $\{v_i\}_{i=1}^M$ corresponding to the M eigenvalues of largest magnitude are calculated. Each eigenvector is normalized so that

$$\|v_i\|^2 = \frac{1}{\lambda_i}. \tag{14}$$

The orthonormal POD basis set $\{\phi_i(\mathbf{x})\}_{i=1}^M$ is constructed according to

$$\phi_i(\mathbf{x}) = \sum_{j=1}^N v_{i,j} S_j(\mathbf{x}), \tag{15}$$

where $v_{i,j}$ is the j^{th} component of v_i. The POD basis is optimal in an energy sense.[21] It captures the mean square energy of the snapshot ensemble better than any other basis.

With the basis in hand, the system solution $w(t,\mathbf{x})$ is approximated as a linear combination of POD modes, i.e.,

$$w(t,\mathbf{x}) \approx \sum_{i=1}^M \alpha_i(t)\phi_i(\mathbf{x}). \tag{16}$$

Galerkin projection onto the basis results in a system of ordinary differential equations for the temporal coefficients $\{\alpha_i\}_{i=1}^M$.

Snapshot Decomposition

Using an energy argument based on (13) is a convenient way to determine the number of POD modes needed for the reduced model. However, blindly applying (13) to determine the necessary number of modes is problematic in a feedback control setting. First, the snapshot ensemble typically consists of baseline (zero control input) and actuated data. Actuated data is obtained by stimulating the system with open-loop control inputs. Using an energy argument based on open-loop information to make conclusions about the energy of the system under feedback control is problematic. The energy content of open-loop data is likely very different than the energy content of the system under feedback control. Second, in many applications it is possible that energy content in the snapshot ensemble is dominated by that in the baseline data. This is particularly troublesome in the context of boundary control. In boundary control applications, it is usually desired that control input energy be as small as possible while still satisfying the control objective. For example, in flow control applications where the control is located on a surface, it is desired that small control inputs yield large changes in the flow field behavior.[23] In essence, effects of small control inputs are amplified by the natural instabilities and comparatively high energy content of the baseline flow field. Simply applying (13) to an ensemble consisting of baseline and actuated data presents the risk of important structures due to control input being discarded if they are of much lower energy content than structures associated with the baseline solution. For these reasons, we extend the POD algorithm described above so that baseline and control input energy are considered separately. The resulting basis set will consist of modes significant to the baseline solution as well as those significant to the system under control actuation.

The basic idea is to decompose each snapshot in the ensemble into a component in the span of the baseline POD basis and an orthogonal component. This is done by employing useful properties of orthogonal projections on Hilbert spaces.[24] By considering the case of baseline and actuated data separately, the orthogonal component is constructed such that it contains new information due to the control input. This

new information can be used in conjunction with (13) to determine additional modes that are significant from a control standpoint.

An ensemble of solution snapshots is generated for the case of zero control input. From this baseline snapshot ensemble, a set of POD modes is constructed using the snapshot algorithm discussed previously. For notational convenience, denote the baseline basis by $\{\xi_j\}_{j=1}^{M_B}$ where M_B is the total number of baseline modes. By employing the energy ratio in (13), M_B can be chosen such that the baseline basis contains an arbitrary amount of the energy contained in the baseline snapshot ensemble.

With a set of baseline modes in hand, an ensemble of solution snapshots is generated for the case of nonzero control input. Denote the actuated ensemble by $\{T_i\}_{i=1}^{N_A}$ where N_A is the total number of actuated snapshots.

For each snapshot in the actuated ensemble, we determine the component that is in the span of the baseline basis. In particular, define b_{ij} according to

$$b_{ij} = \langle T_i, \xi_j \rangle, 1 \leq i \leq N_A, 1 \leq j \leq M_B. \tag{17}$$

Then, b_{ij} is the projection of the ith actuated snapshot T_i onto the jth baseline POD mode ξ_j. In other words, the product $b_{ij}\xi_j$ is the component of T_i that is in the direction of ξ_j. The linear combination $\sum_{j=1}^{M_B} b_{ij}\xi_j$ is the component of T_i in the span of the baseline basis.

Define $\tilde{T}_i$ according to

$$\tilde{T}_i = T_i - \sum_{j=1}^{M_B} b_{ij}\xi_j. \tag{18}$$

Then, $\tilde{T}_i$ is the component of T_i not contained in the span of the baseline basis. As T_i is a solution snapshot for the case of nonzero control input, $\tilde{T}_i$ consists of new information due to the control input that is not already contained in the span of the baseline modes.

A second set of POD modes is constructed from the data ensemble $\{\tilde{T}_i\}_{i=1}^{N_A}$. Denote this set of "actuator modes" by $\{\eta_i\}_{i=1}^{M_A}$, where M_A is the total number of modes. The energy ratio in (13) is used to determine M_A such that the basis of actuator modes contains an arbitrary amount of the additional energy resulting from the control input.

By construction, the set of baseline modes consists of orthonormal basis functions. Similarly, the actuator modes are orthonormal. It is easy to show that the set of baseline modes is orthogonal to the set of actuator modes. Consider the inner product of ξ_k and $\tilde{T}_i$ for arbitrary i, k. We see that

$$\left\langle \tilde{T}_i, \xi_k \right\rangle = \left\langle T_i - \sum_{j=1}^{M_B} b_{ij}\xi_j, \xi_k \right\rangle \tag{19}$$

$$= \langle T_i, \xi_k \rangle - \sum_{j=1}^{M_B} b_{ij} \langle \xi_j, \xi_k \rangle. \tag{20}$$

As the baseline modes are orthonormal, $\langle \xi_j, \xi_k \rangle = 0$ unless $j = k$. For $j = k$, $\langle \xi_j, \xi_k \rangle = 1$. As a result,

$$\langle T_i, \xi_k \rangle - \sum_{j=1}^{M_B} b_{ij} \langle \xi_j, \xi_k \rangle = \langle T_i, \xi_k \rangle - b_{ik}. \tag{21}$$

By definition (17), $b_{ik} = \langle T_i, \xi_k \rangle$. Thus, we have

$$\left\langle \tilde{T}_i, \xi_k \right\rangle = 0, \text{ for arbitrary } i, k. \tag{22}$$

From (15), each actuator mode η_i is a linear combination of the snapshots $\{\tilde{T}_i\}_{i=1}^{N_A}$. As a result, (22) in combination with the linearity of the inner product yields

$$\langle \eta_i, \xi_k \rangle = 0, \text{ for arbitrary } i, k. \tag{23}$$

Therefore, we have

$$\{\eta_i\} \perp \{\xi_j\}. \tag{24}$$

This result allows us to combine the baseline and actuator modes into an overall basis set

$$\{\phi_i\}_{i=1}^{M_B+M_A} = \{\xi_1, \xi_2, ..., \xi_{M_B}, \eta_1, \eta_2, ..., \eta_{M_A}\}, \tag{25}$$

where all modes in the basis are orthonormal. This is advantageous for the development of reduced order models. The system solution $w(t, \mathbf{x})$ is still approximated as a linear combination of modes as in (16). Moreover, separate consideration of baseline and actuated energy allows us to write this linear combination as

$$w(t, \mathbf{x}) \approx \sum_{j=1}^{M_B} \theta_j(t)\xi_j(\mathbf{x}) + \sum_{i=1}^{M_A} \beta_i(t)\eta_i(\mathbf{x}), \tag{26}$$

where $\{\theta_j\}_{j=1}^{M_B}$ and $\{\beta_i\}_{i=1}^{M_A}$ are temporal coefficients for the baseline and actuator basis, respectively. This allows us to consider the system solution as a baseline component and an additional component induced by the control input.

Reduced Order Model

We now develop a reduced order model for the system described by (3), (5)-(10). Our aim is to develop a low order state-space model where the Dirichlet control inputs specified by (5)-(6) appear in the model explicitly.

Taking the inner product of both sides of (3) with the ith POD mode $\phi_i(x, y)$ and utilizing Green's identities results in the weak formulation

$$\begin{aligned}\int_\Omega \frac{\partial}{\partial t} w(t, x, y)\phi_i(x, y)\mathbf{dx} = \frac{1}{Re}\left[\int_{\partial\Omega} (\nabla w(t, x, y) \cdot \mathbf{n})\phi_i(x, y)dA(\mathbf{x}) - \int_\Omega \nabla w(t, x, y) \cdot \nabla\phi_i(x, y)\mathbf{dx}\right] \\ - \left[\int_{\partial\Omega} (F(w) \cdot \mathbf{n})\phi_i(x, y)dA(\mathbf{x}) - \int_\Omega F \cdot \nabla\phi_i(x, y)\mathbf{dx}\right],\end{aligned} \tag{27}$$

where $\mathbf{n}$ denotes the unit outward normal.

As seen in (15), each POD mode is a linear combination of solution snapshots. From (9), snapshot values along Γ_U are specified to be zero. As a result, POD modes are zero along Γ_U. Thus, the first boundary integral in (27) is decomposed as

$$\begin{aligned}&\int_{\partial\Omega} (\nabla w(t, x, y)\cdot\mathbf{n})\phi_i(x, y)dA(\mathbf{x}) \\ &\quad = \int_{a_1}^{a_2} \left(\frac{\partial}{\partial y} w(t, x, b_1)\phi_i(x, b_1) - \frac{\partial}{\partial y} w(t, x, b_2)\phi_i(x, b_2)\right) dx - \int_c^d \frac{\partial}{\partial x} w(t, a, y)\phi_i(a, y)dy,\end{aligned} \tag{28}$$

where condition (8) has been used to specify that

$$\int_c^d \frac{\partial}{\partial x} w(t, b, y)\phi_i(b, y)dy = 0. \tag{29}$$

In a similar fashion, the remaining boundary integral in (27) is decomposed as

$$\int_{\partial\Omega} (F(w) \cdot \mathbf{n})\phi_i(x, y)dA(\mathbf{x}) = \frac{1}{2}\int_c^d \left(w(t, b, y)^2\phi_i(b, y) - f(y)^2\phi_i(a, y)\right) dy, \tag{30}$$

where (7) has been used to incorporate the inflow condition $f(y)$.

Control inputs and the Dirichlet inflow condition are not explicit in (28). They can be made explicit by approximating partial derivatives along the boundary. For $h > 0$, we see that

$$\frac{\partial}{\partial y} w(t, x, b_1) \approx \frac{u_B(t)\Psi_B(x) - w(t, x, b_1 - h)}{h}, \tag{31}$$

$$\frac{\partial}{\partial y} w(t, x, b_2) \approx \frac{w(t, x, b_2 + h) - u_T(t)\Psi_T(x)}{h}, \tag{32}$$

$$\frac{\partial}{\partial x} w(t, a, y) \approx \frac{w(t, a + h, y) - f(y)}{h}. \tag{33}$$

These expressions are substituted into (28). Approximating $w(t,x,y)$ as a linear combination of POD modes in (27), (28), and (30) results in a reduced order system model. This system is of the form

$$\dot{\alpha} = A\alpha + Bu + G(\alpha) + F, \tag{34}$$

where

$$\begin{aligned} A(i,j) = -\frac{1}{hRe}[&\int_{a_1}^{a_2} (\phi_j(x,b_1-h)\phi_i(x,b_1) + \phi_j(x,b_2+h)\phi_i(x,b_2))dx \\ &+ \int_c^d \phi_j(a+h,y)\phi_i(a,y)dy + h\int_\Omega \nabla\phi_i(x,y)\cdot\nabla\phi_j(x,y)]\mathbf{dx}, \end{aligned} \tag{35}$$

$$B = \frac{1}{hRe}\begin{bmatrix} \int_{a_1}^{a_2}\phi_1(x,b_1)\Psi_B(x)dx & \int_{a_1}^{a_2}\phi_1(x,b_2)\Psi_T(x)dx \\ \cdot & \cdot \\ \cdot & \cdot \\ \cdot & \cdot \\ \int_{a_1}^{a_2}\phi_M(x,b_1)\Psi_B(x)dx & \int_{a_1}^{a_2}\phi_M(x,b_2)\Psi_T(x)dx \end{bmatrix}_{M\times 2}, \tag{36}$$

$$G(\alpha) = \frac{1}{2}\begin{bmatrix} \int_\Omega \left(\sum_{j=1}^M \alpha_j\phi_j(x,y)\right)^2 \frac{\partial}{\partial x}\phi_1(x,y)\mathbf{dx} - \int_c^d \left(\sum_{j=1}^M \alpha_j\phi_j(b,y)\right)^2 \phi_1(b,y)dy \\ \cdot \\ \cdot \\ \cdot \\ \int_\Omega \left(\sum_{j=1}^M \alpha_j\phi_j(x,y)\right)^2 \frac{\partial}{\partial x}\phi_M(x,y)\mathbf{dx} - \int_c^d \left(\sum_{j=1}^M \alpha_j\phi_j(b,y)\right)^2 \phi_M(b,y)dy \end{bmatrix}_{M\times 1}, \tag{37}$$

$$F = \begin{bmatrix} \int_c^d (\frac{1}{hRe}f(y) + \frac{1}{2}f(y)^2)\phi_1(a,y)dy \\ \cdot \\ \cdot \\ \cdot \\ \int_c^d (\frac{1}{hRe}f(y) + \frac{1}{2}f(y)^2)\phi_M(a,y)dy \end{bmatrix}_{M\times 1}, \tag{38}$$

$$u = \begin{bmatrix} u_B(t) \\ u_T(t) \end{bmatrix}_{2\times 1}. \tag{39}$$

Projecting the initial condition $w_0(x,y)$ onto the POD basis results in an initial condition for the reduced order model of the form

$$\alpha(0) = \alpha_0. \tag{40}$$

Open-Loop Comparisons

We now demonstrate the impact of basis construction technique on the ability of the reduced model to represent dynamics induced by a boundary control input. Instantaneous snapshots are generated for (3), (5)-(10) via numerical simulation. A positive parabolic profile with unit maximum amplitude is specified for the inlet condition in boundary condition (7). In (4), we set $C_1 = 1$ and $C_2 = 0$ in order to obtain solutions that convect from left to right for the positive inlet. In addition, we specify that $Re = 300$. The problem domain Ω is discretized, resulting in a uniform grid with spatial step-size h. We utilize a finite difference scheme[25] to numerically solve the model problem with and without boundary control input. The resulting discretized system describes roughly 2,000 states.

We construct reduced order models from snapshot ensembles obtained for two scenarios. In the first scenario, snapshots are generated for the baseline solution and for boundary actuation at a fixed frequency. For the second case, snapshots are generated for the baseline solution and a more complicated boundary input where the frequency varies with time. For both scenarios, we compare model agreement resulting from combining baseline and actuator snapshots into an overall lumped snapshot ensemble to that obtained by decomposing snapshots into their baseline and actuated components and constructing the POD basis as in (25). In the results that follow, basis construction from a lumped snapshot ensemble is referred to as the "lumped" method. Constructing the basis by considering baseline and actuated energy separately is referred to as the "split" method.

Scenario 1

Snapshots are generated for the baseline solution and for the solution arising under periodic boundary actuation. Inputs specified are of the form

$$u_B(t) = sin(\pi t) \qquad u_T(t) = 0, \tag{41}$$

$$u_B(t) = 0 \qquad u_T(t) = sin(\pi t). \tag{42}$$

In (41), periodic actuation is done on the bottom of the obstacle while values along the obstacle top are held at zero. In (42), values along the obstacle bottom are held at zero with periodic actuation occurring at the top. For each control input listed in (41)-(42), snapshots are taken in increments of $\Delta t = 0.1$ starting from $t = 0$ and ending at $t = 15$. The steady baseline solution is used for the initial condition.

With an ensemble of snapshots in hand, ratio (13) is used to determine the number of basis modes to construct. Requiring that 99.9% of the ensemble energy be contained in the POD basis results in a lumped basis consisting of 7 modes. Separate consideration of baseline and actuated energy results in a split basis consisting of 1 baseline mode and 16 actuator modes.

We now employ linear combination (16) to compare boundary condition agreement between the full order system and reduced models obtained via the lumped and split POD bases. By specifying characteristic functions for the control profiles $\Psi_B(x)$ and $\Psi_T(x)$ in (5)-(6), we see that

$$\sum_{i=1}^{M} \alpha_i(t)\phi_i(\Gamma_B) \approx w(t, \Gamma_B) = u_B(t), \tag{43}$$

$$\sum_{i=1}^{M} \alpha_i(t)\phi_i(\Gamma_T) \approx w(t, \Gamma_T) = u_T(t), \tag{44}$$

We construct the linear combinations on the left in (43)-(44) and compare them to the exact boundary conditions $u_B(t)$ and $u_T(t)$ specified in the full order system. We first perform comparisons for boundary inputs explicitly used during ensemble generation. Results obtained for the baseline solution and for the solution with periodic boundary actuation of the form $sin(\pi t)$ are shown in Figure 2. In that figure, dashed curves denote the linear combination of POD modes restricted to the boundary. Solid curves denote the exact full order boundary input. Results obtained for the lumped basis method are plotted on the left. Split POD basis results are plotted on the right. As seen in Figure 2, both methods result in very good agreement between the exact boundary conditions and the linear combination of POD modes restricted to the boundary. Dashed and solid curves are virtually identical.

In a feedback control setting, dynamics induced by the control are typically not known a priori. It is not possible to specify a boundary feedback control law as an open-loop input during ensemble creation. The specifics of the control law and the dynamics induced by it are not known at that stage. Typically, in the closed-loop system, the boundary input resulting from the control law will be different than the inputs used to generate the snapshot ensemble. As a result, it is useful to compare reduced and full order model agreement for inputs not specified during ensemble creation. This provides insight into the suitability of the reduced model for closed-loop control law design. For these reasons, we now compare boundary condition agreement between the reduced and full order systems for open-loop inputs that were not used during ensemble creation.

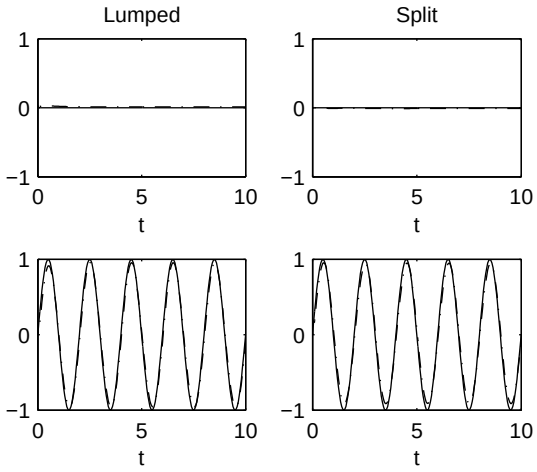

Figure 2: Boundary Condition Accuracy.

Boundary inputs specified are of the form

$$u_B(t) = min\left(\frac{t}{3}, 1\right), \tag{45}$$

$$u_T(t) = sin\left(\frac{3}{2}\pi t\right). \tag{46}$$

Results obtained for the lumped and split basis methods are shown in Figure 3.

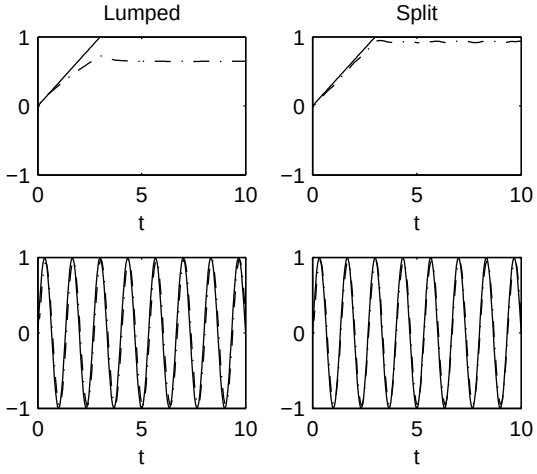

Figure 3: Boundary Condition Accuracy.

As seen in Figure 3, very good agreement is seen between the reduced and full order systems for the split method, even though the inputs considered were not specifically included in the snapshot ensemble. Condition (46) is reconstructed well using the lumped method. However, the reconstruction of the piecewise linear input in (45) is much less accurate when the lumped basis is used.

To further compare the lumped and split basis methods and their utility for control law design, we project the full order solution at each time step onto the lumped and split POD bases. The resulting temporal coefficients are compared to those predicted by the reduced order models. Boundary inputs specified are as in (45)-(46). Results obtained for the first 5 temporal coefficients of the lumped method are shown in Figure 4. The first 5 temporal coefficients for the split method are shown in Figure 5. In Figures 4-5,

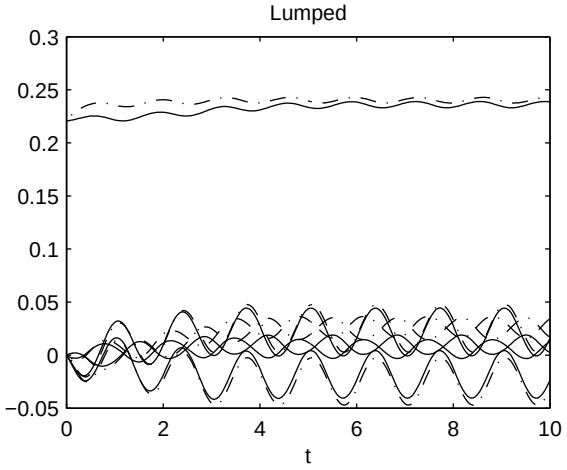

Figure 4: Temporal Coefficient Accuracy for the Lumped Method.

solid curves denote values of temporal coefficients obtained via the projection. Dashed curves denote the solution of the reduced order model. Overall, the accuracy of the split method is better, particularly for temporal coefficients with higher frequency content. Separate consideration of actuated energy during basis construction results in better representation of dynamics induced by boundary inputs not specified during ensemble creation. This is advantageous in a boundary feedback control setting where dynamics induced by the control are typically not known beforehand.

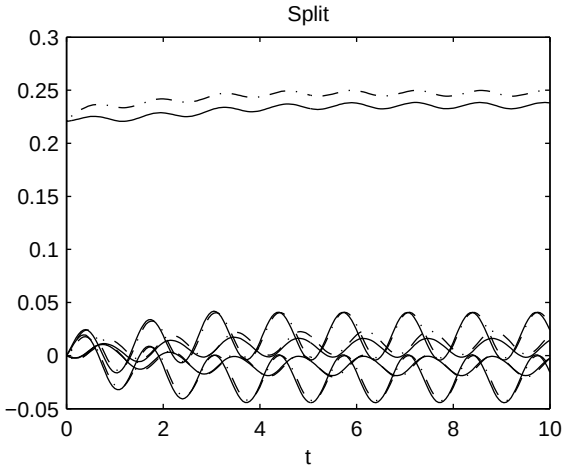

Figure 5: Temporal Coefficient Accuracy for the Split Method.

Scenario 2

It is likely that a snapshot ensemble for inputs at a single frequency results in a POD basis that does not adequately span the dynamics induced by a feedback control. Feedback controls designed from such a basis are bound to be ineffective when implemented in the full order system. In Scenario 2, we compare the lumped and split basis methods using a snapshot ensemble generated from boundary inputs that excite a range of system dynamics. Inputs specified are of the form

$$u_B(t) = sin\left(\pi\left(e^t\right)^{0.3}\right) \qquad u_T(t) = 0, \tag{47}$$

$$u_B(t) = 0 \qquad u_T(t) = sin\left(\pi\left(e^t\right)^{0.3}\right). \tag{48}$$

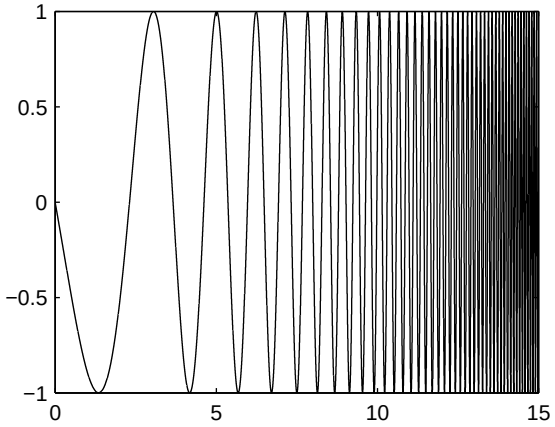

Figure 6: The input function $u = sin\left(\pi\left(e^t\right)^{0.3}\right)$.

The sinusoidal input function is shown in Figure 6. As seen in that figure, an input of this form generates the system response over a range of frequencies. The resulting POD basis is much more likely to adequately span the unknown dynamics generated by a feedback control.

Instantaneous snapshots are generated for the baseline solution as well as for solutions arising from the inputs in (47)-(48). For each control input listed in (47)-(48), snapshots are taken in increments of $\Delta t = 0.1$ starting from $t = 0$ and ending at $t = 15$. The steady baseline solution is used for the initial condition.

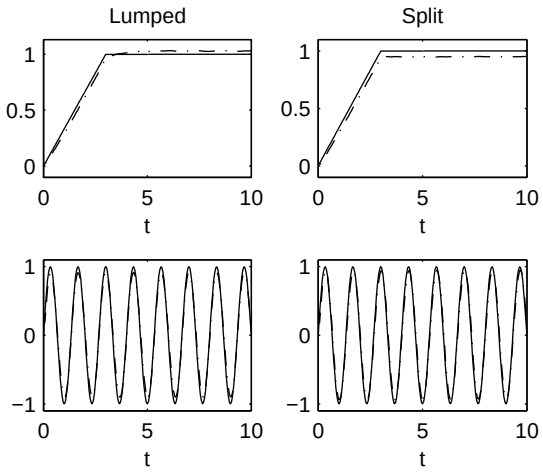

Figure 7: Boundary Condition Accuracy.

Requiring that 99.9% of the ensemble energy be contained in the POD basis results in a lumped basis consisting of 7 modes. A split basis comprised of 1 baseline mode and 25 actuator modes are needed when baseline and actuated energy is considered separately.

As in Scenario 1, we compare boundary condition accuracy of the lumped and split methods for boundary inputs not specified during ensemble generation. For the sake of comparison, we use the boundary conditions given by (45)-(46). Results obtained for the lumped and split basis methods are shown in Figure 7. As seen in that figure, very good boundary condition agreement is seen between the reduced and full order systems for both basis methods. In particular, by comparing Figures 3 and 7, we see that the piecewise linear boundary condition in (45) is represented much better by the lumped method when inputs (47)-(48) are used to generate the snapshot ensemble.

As before, we now project the full order solution at each time step onto the lumped and split POD bases. The resulting temporal coefficients are compared to those predicted by the reduced order models. The

results for the lumped method are shown in Figure 8. Split method results are shown in Figure 9. As seen in those figures, the accuracy of the split method is better. For temporal coefficients with significant frequency content, values predicted by the reduced model are virtually identical to those obtained by projecting the full solution onto the split basis, even though the boundary inputs specified are different than those used during ensemble creation. The split method is better suited with regard to feedback control law design as it is more capable of accurately representing dynamics that are not explicitly included in the snapshot ensemble.

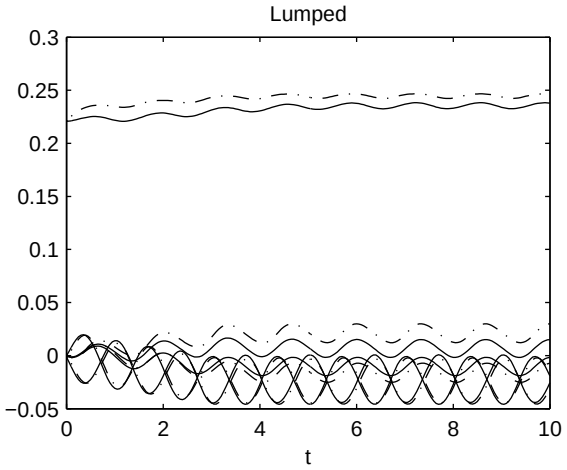

Figure 8: Temporal Coefficient Accuracy for the Lumped Method.

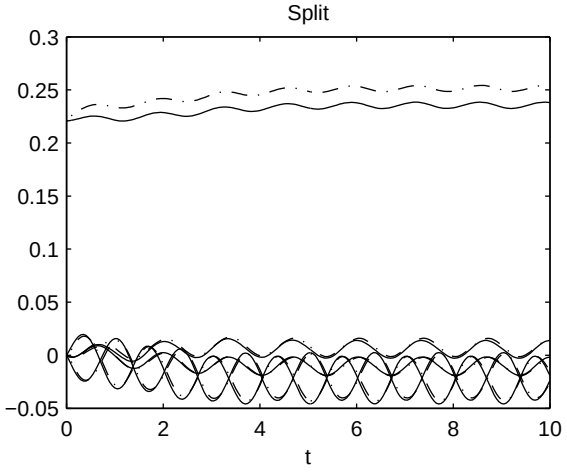

Figure 9: Temporal Coefficient Accuracy for the Split Method.

Control Formulation

We now specify the control formulation used to compare the effectiveness of the lumped and split basis methods in a feedback control setting. The reduced system given by (34), (40) is linearized about the origin yielding a state-space equation of the form

$$\dot{\alpha}(t) = A\alpha + Bu, \tag{49}$$

$$\alpha(0) = \alpha_0. \tag{50}$$

We consider the tracking problem for (49)-(50). A fixed reference signal $w_{ref}(\mathbf{x})$ is specified for the full order system. Projecting $w_{ref}(\mathbf{x})$ onto the POD basis yields tracking coefficients for the reduced order

model, denoted by α_{ref}. The dynamics of the linearized model under tracking control are given by

$$\begin{bmatrix} \dot{\alpha} \\ \alpha_{ref} \end{bmatrix} = \begin{bmatrix} A & 0 \\ 0 & 0 \end{bmatrix} \begin{bmatrix} \alpha \\ \alpha_{ref} \end{bmatrix} + \begin{bmatrix} B \\ 0 \end{bmatrix} u \tag{51}$$

$$= \bar{A}X + \bar{B}u, \tag{52}$$

where we have defined the augmented state X as

$$X(t) = \begin{bmatrix} \alpha(t) \\ \alpha_{ref} \end{bmatrix} \text{ with } X_0 = \begin{bmatrix} \alpha_0 \\ \alpha_{ref} \end{bmatrix}. \tag{53}$$

To formulate the control problem, we consider the γ-shifted linear quadratic regulator (LQR) cost function

$$J(\alpha_0, u) = \int_0^\infty \left\{ (\alpha - \alpha_{ref})^T Q (\alpha - \alpha_{ref}) + u^T R u \right\} e^{2\gamma t} dt. \tag{54}$$

In (54), Q is a diagonal, symmetric, positive semi-definite matrix of state weights. R is a diagonal, symmetric, positive definite matrix of control weights. The quantity γ, a nonnegative constant, is an additional parameter that provides added robustness in the control.[26,27] The optimal control problem we consider is to minimize (54) over all controls $u \in L^2(0, \infty)$ subject to the constraints (51)-(53).

For a controllable system, the LQR problem has a unique solution of the form

$$u_{opt} = -KX \tag{55}$$

$$= -[K_1 \quad K_2]X \tag{56}$$

$$= -\left[R^{-1}B^T\Pi_{11} \quad R^{-1}B^T\Pi_{12}\right] X, \tag{57}$$

where Π_{11} is the unique symmetric, non-negative solution of the algebraic Riccati equation

$$(A + \gamma I)^T \Pi_{11} + \Pi_{11}(A + \gamma I) - \Pi_{11} B R^{-1} B^T \Pi_{11} + Q = 0. \tag{58}$$

The matrix Π_{12} in (57) satisfies the equation

$$\left[(A + \gamma I)^T - \Pi_{11} B R^{-1} B^T\right] \Pi_{12} = Q. \tag{59}$$

The feedback control obtained from the linearized model is placed into the nonlinear state-space equation. The resulting closed-loop nonlinear system is of the form

$$\dot{X} = (\bar{A} - \bar{B}K)X + [G(\alpha)\ 0]^T + [F\ 0]^T, \tag{60}$$

$$X(0) = X_0. \tag{61}$$

Closed-Loop Results

We use the LQR formulation in (54) to compare closed-loop results obtained from the lumped and split basis methods. A snapshot ensemble is constructed containing baseline solution data as well as data resulting from nonzero boundary actuation. As it is desired that the POD basis spans unknown dynamics introduced by the LQR feedback control, boundary inputs specified during ensemble creation are of the form

$$u_B(t) = C sin\left(\pi \left(e^t\right)^{0.3}\right) \qquad u_T(t) = 0, \tag{62}$$

$$u_B(t) = 0 \qquad u_T(t) = C sin\left(\pi \left(e^t\right)^{0.3}\right) \tag{63}$$

for $C = 1, 2, 3$.

For each control input listed in (62)-(63), snapshots are taken in increments of $\Delta t = 0.1$ starting from $t = 0$ and ending at $t = 15$. The steady baseline solution is specified for the initial condition. The resulting snapshot ensemble consists of roughly 900 snapshots. Requiring that 99% of the ensemble energy be contained in the POD basis results in a lumped basis consisting of 5 modes. A split basis comprised of 1 baseline mode and 20 actuator modes is needed when baseline and actuated energy are considered separately. The first 9

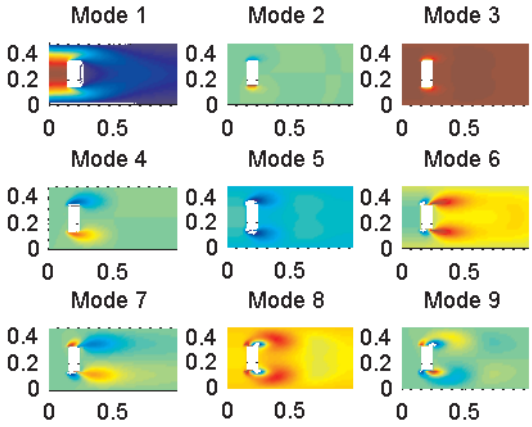

Figure 10: Split Basis Modes.

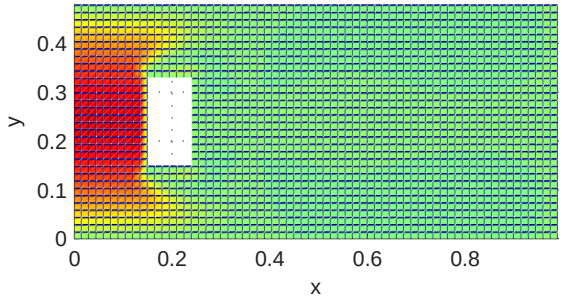

Figure 11: Tracking Reference Function.

modes of the split basis are shown in Figure 10. In that figure, mode 1 is the baseline mode. Modes 2-9 are actuator modes.

The tracking LQR problem requires the specification of the reference signal α_{ref}. In the results that follow, α_{ref} is obtained from the unactuated steady solution for the case $Re = 50$. This solution is projected onto the lumped and split bases. The temporal values obtained are used as tracking coefficients in the reduced order control problem. The reference signal obtained by projecting the steady solution at $Re = 50$ onto the split basis is shown in Figure 11. The reference function obtained by projecting onto the lumped basis is similar. To complete the control formulation, each state in the reduced order model is prescribed a weight of 2,500. The two boundary controls are each given unit weight. The value specified for γ in (54) is 0.25. The closed-loop solution of the reduced order model constructed with the split POD basis is shown in Figure 12. By comparing the controlled solution of Figure 12 to the reference function in Figure 11, it is apparent that the closed-loop reduced order model satisfies the control objective quite well. Separate consideration of actuated energy in the split POD basis method results in satisfactory tracking of the reference signal.

When the energy ratio in (13) is applied to baseline and actuated data lumped together into an overall snapshot ensemble, the results are much less favorable. Closed-loop solutions of the reduced order model constructed with the lumped POD basis are shown in Figure 13. As seen in that figure, virtually no tracking is achieved by the reduced order control. Adjusting parameters in the control formulation has little effect on this result. Increasing the state-weights and the parameter γ to 10,000 and 0.75, respectively, does not significantly improve the performance of the control. System information relevant from a control standpoint is discarded when an energy argument is applied during order reduction to the lumped snapshot ensemble containing baseline and actuated data. The resulting reduced order model does not adequately describe

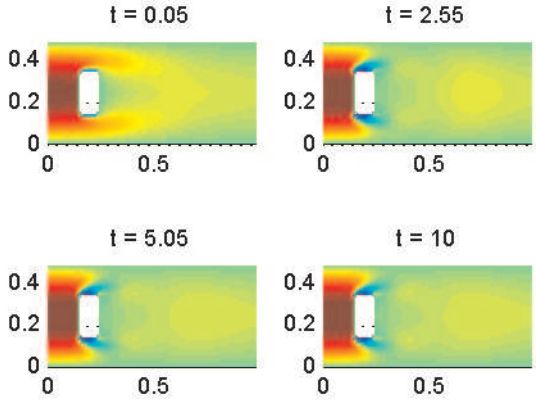

Figure 12: Closed-Loop Split Model.

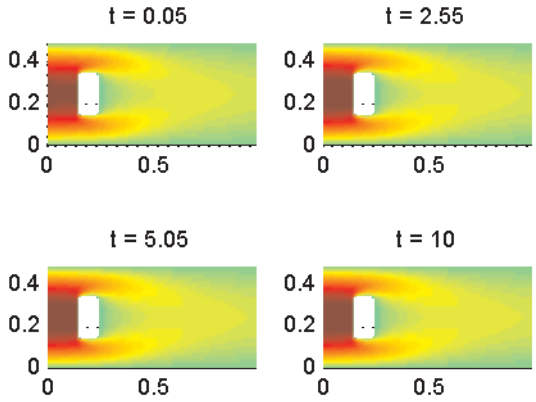

Figure 13: Closed-Loop Lumped Model.

dynamics induced by the control. Consequently designing a feedback control from such a model results in very ineffective response when the control is applied to the system.

Full Order Validation

To validate the effectiveness of the reduced order control obtained via the split basis method, we utilize a fixed-point projection algorithm[16] to incorporate the reduced order boundary control in the full order model. The closed-loop solution of the full order system is shown in Figure 14. As seen in that figure, the reduced order control effectively drives the full order plant to the target profile. The full order discretized model is comprised of roughly 2,000 states. The reduced model obtained via the split basis method describes 21 states. As a result, system dimension is reduced by roughly two orders of magnitude with the resulting reduced order control being quite effective.

Conclusions

In this paper, a reduced basis construction method was developed allowing for separate consideration of baseline and actuated dynamics in the reduced modeling process. A prototype initial boundary value problem, governed by the two-dimensional Burgers equation, was formulated to demonstrate the utility of the method. A weak formulation approach was used to develop a reduced order model of the system with boundary control appearing explicitly in the reduced model. When actuated energy was considered

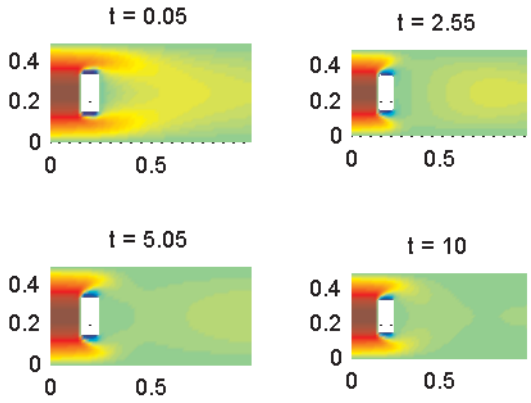

Figure 14: Closed-Loop Response with Split Method Feedback Control.

separately, much better agreement was seen between open-loop solutions of the reduced and full order systems. Separate consideration of energy induced by the boundary control resulted in effective feedback control for the reduced and full order systems. When actuated energy was not explicitly accounted for in the reduced modeling process, the resulting feedback control was completely ineffective when applied to the system.

These results demonstrate the need for separate consideration of baseline and actuated energy in the reduced modeling process when the resulting model is to be used for feedback control law design. Basis construction relying on an energy argument applied to a lumped snapshot ensemble containing baseline and actuated data can result in important control information being discarded during order reduction. This is particularly the case in a boundary control setting where ensemble energy is typically dominated by that in the baseline data. Feedback controls developed from the resulting reduced model are likely ineffective when applied to the system. Separate consideration of dynamics induced by boundary control input results in reduced order controllers that are much more effective when applied to the reduced and full order systems.

References

[1] Anderson, J., *Computational Fluid Dynamics*, McGraw-Hill, New York, 1995, pp. 3-31.

[2] Kirk, D., *Optimal Control Theory*, Dover Publications, New York, 2004, pp. 90-93.

[3] Antoulas, A., *Approximation of Large-Scale Dynamical Systems*, Society for Industrial and Applied Mathematics, Philadelphia, 2005, pp. 2-24.

[4] Atwell, J. and King, B., "Computational Aspects of Reduced Order Feedback Controllers for Spatially Distributed Systems," *Proceedings of the 38th IEEE Conference on Control and Desicion*, December 1999, pp. 4301-4306.

[5] Ausseur, J., Pinier, J., Glauser, M., and Higuchi, H., "Experimental Development of a Reduced Order Model for Flow Sepapration Control ," AIAA Paper 2006-1251, January 2006.

[6] Ausseur, J., Pinier, J., and, Glauser, M., "Flow Separation Control Using a Convection Based POD Approach ," AIAA Paper 2006-3017, June 2006.

[7] Banks, H., del Rosario, R., and Smith, R., "Reduced Order Model Feedback Control Design: Numerical Implentation in a Thin Shell Model," Technical Report CRSC-TR98-27, Center for Research in Scientific Computation, North Carolina State University, June, 1998.

[8] Caraballo, E., Samimy, M., and DeBonis, J., "Low Dimensional Modeling of Flow for Closed-Loop Flow Control," AIAA Paper 2003-0059, January 2003.

[9] Caraballo, E., Yuan, X., Little, J., Debaisi, M., Serrani, A., Myatt, J., and Samimy, M., "Further Development of Feedback Control of Cavity Flow Using Experimental Based Reduced Order Model ," AIAA Paper 2006-1405, January 2006.

[10] Cohen, K., Siegel, S., McLaughlin, T., and Myatt, J., "Proper Orthogonal Decomposition Modeling of a Controlled Ginzburg-Landau Cylinder Wake Model," AIAA Paper 2003-2405, January 2003.

[11] Cohen, K., Siegel, S., Seidel, J., and, McLaughlin, T., "Reduced Order Modeling for Closed-Loop Control of Three Dimensional Wakes," AIAA Paper 2006-3356, June 2006.

[12] Efe, M. and Ozbay, H., "Proper Orthogonal Decomposition for Reduced Order Modeling: 2D Heat Flow," *Proc. of 2003 IEEE Conference on Control Applications*, June 23-25, 2003, pp. 1273-1277.

[13] Luchtenburg, M., Tadmore, G., Lehmann, O., Noack, B., King, R., and Morzynski, M., "Tuned POD Galerkin Models for Transient Feedback Regulation of the Cylinder Wake," AIAA Paper 2006-1407, January 2006.

[14] Siegel, S., Cohen, K., Seidel, J., and, McLaughlin, T., "Proper Orthogonal Decomposition Snapshot Selection for State Estimation of Feedback Controlled Flows ," AIAA Paper 2006-1400, January 2006.

[15] Bensoussan, A., Prato, G., Delfour, M., and Miller, S., "Representation and Control of Infinite Dimensional Systems," Vol. 2 of *Systems & Control: Foundations & Applications*, Birkhauser, Boston, 1992, pp. 259-317.

[16] Camphouse, R.C., "Boundary Feedback Control Using Proper Orthogonal Decomposition Models," *Journal of Guidance, Control, and Dynamics*, Vol. 28, No. 5, September-October 2005, pp 931-938.

[17] Camphouse, R. C. and Myatt, J. H., "Reduced Order Modelling and Boundary Feedback Control of Nonlinear Convection," AIAA Paper 2005-5844, August 2005.

[18] Carlson, H., Glauser, M., Higuchi, H., and Young, M., "POD Based Experimental Flow Control on a NACA-4412 Airfoil," AIAA Paper 2004-0575, January 2004.

[19] Carlson, H., Glauser, M., and Roveda, R., "Models for Controlling Airfoil Lift and Drag," AIAA Paper 2004-0579, January 2004.

[20] Batchelor, G., *An Introduction to Fluid Dynamics*, Cambridge University Press, New York, 1999, pp. 147.

[21] Holmes, P., Lumley, J., and Berkooz, G., *Turbulence, Coherent Structures, Dynamical Systems and Symmetry*, Cambridge University Press, New York, 1996, pp. 86-127.

[22] Sirovich, L., "Turbulence and the Dynamics of Coherent Structures, Parts I-III," *Quarterly of Applied Mathematics*, Volume 45, Brown University, Rhode Island, 1987, pp. 561-590.

[23] Gad el Hak, M., *Flow Control: Passive, Active, and Reactive Flow Management*, Cambridge University Press, New York, 2000, pp. 318-357.

[24] Debnath, L. and Mikusiński, P., *Introduction to Hilbert Spaces with Applications*, Academic Press, California, 1999, pp. 87-130.

[25] Camphouse, R. and Myatt, J., "Feedback Control for a Two-Dimensional Burgers Equation System Model," AIAA Paper 2004-2411, June 2004.

[26] Burns, J. and Kang, S., "A Control Problem for Burgers Equation with Bounded Input/Output," *Nonlinear Dynamics*, Volume 2, Kluwer Academic Publishing, New York, 1991, pp. 235-262.

[27] Burns, J. and Kang, S., "A Stabilization Problem for Burgers Equation with Unbounded Control and Observation," *Control and Estimation of Distributed Parameter Systems*, Volume 100, Birkhauser Verlag, Basel, 1991, pp. 51-72.